Chinese Chemical Letters 37 (2026) 111554

Contents lists available at ScienceDirect

Chinese Chemical Letters

journal homepage: www.elsevier.com/locate/cclet

Self-assembled chiral cages for anion recognition

Ze Cao[a,1], Chenqi Ge[a,1], Yating Wu[a], Hua Tang[a], Yueyan Kuang[a], Yuyang Wu[a], Hao Li[a,b,*]

[a] Department of Chemistry, Zhejiang University, Hangzhou 310058, China
[b] ZJU-Hangzhou Global Scientific and Technological Innovation Center, Zhejiang University, Hangzhou 311200, China

ARTICLE INFO

Article history:
Received 20 April 2025
Revised 20 June 2025
Accepted 7 July 2025
Available online 8 July 2025

Keywords:
Self-assembly
Chiral cage
Dynamic covalent bond
Anion recognition

ABSTRACT

In this study, two chiral cationic cage-shaped hosts were successfully self-assembled *via* imine condensation, achieving near-quantitative yields. Compared with the counterparts bearing a single imine bond, the intrinsic multivalency of the cage frameworks confers significant robustness to the cages, even when exposed to aqueous environments. Each cage features three relatively acidic CH protons oriented towards the interior cavity or clefts, enabling the efficient recognition of anionic guests through cooperative hydrogen bonding. The cage containing pyridinium functions adopts a *pseudo* face-in conformation, thus it accommodates anionic guests in its peripheral windows in a 1:2 stoichiometry. As a comparison, the cage containing imidazolium functions adopts an edge-in conformation, and thus recognizes the anions within the cavity in a 1:1 binding stoichiometry.

© 2025 Published by Elsevier B.V. on behalf of Chinese Chemical Society and Institute of Materia Medica, Chinese Academy of Medical Sciences.

Anion detection has proven to be of significant importance due to the critical roles these negatively charged species play in nature. Anions are involved in mediating essential processes such as metabolic regulation [1–3], aquatic eutrophication [4–6], and the maintenance of physiological homeostasis [7–10]. A widely adopted strategy for anion recognition involves designing macrocyclic hosts with intrinsic cavities that can accommodate anionic guests through noncovalent interactions, particularly hydrogen bonding, in a synergistic manner [11–15]. Recently, inspired by the enhanced binding affinities of cryptands toward cationic guests compared to their two-dimensional counterparts (*e.g.*, crown ethers) [16,17], chemists have discovered that cage-shaped molecules often exhibit stronger anion-binding capabilities than macrocyclic analogues [18–24]. A notable example of this was reported by Flood and co-workers, who synthesized a cage, *via* a click reaction, that was capable of extracting chloride anions from aqueous solution [25]. However, a frequent drawback of these irreversible synthetic approaches is the generation of oligomeric or polymeric byproducts during the formation of the target cage molecules.

Reversible covalent reactions provide a promising alternative by enabling error correction during self-assembly [26–30]. Nevertheless, this dynamic nature can compromise the robustness of the self-assembled molecules. For instance, acceptors containing imine bonds, a commonly used dynamic covalent bond, are prone to hydrolysis in aqueous media [31–33]. Therefore, the development of synthetic strategies that balance the error-correcting benefits of reversible reactions with high product stability remains a key challenge. As demonstrated in prior research [34], a cage-shaped molecule was synthesized in near-quantitative yield by condensing a triscationic hexaformyl precursor with three equivalents of bisamine linker. Despite the presence of six imine bonds in its framework, the cage exhibits remarkable kinetic stability against hydrolysis in aqueous media, compared with those compounds each contains only one single imine bond. This stability arises from the fact that disrupting one of the three bisamino building blocks requires breaking two imine bonds simultaneously, a process that is significantly more energy-demanding than cleaving a single bond. Leveraging the hydrophobic effect, the cage can encapsulate alkane derivatives within its intrinsic cavity, where all the aromatic building blocks in the cage framework are oriented in a face-in configuration. Building on this, we hypothesize that by reorienting the cationic pyridinium units into an edge-in arrangement, the cage could potentially recognize anionic guests through hydrogen bonding interactions.

Herein, we report the self-assembly of two structurally analogous chiral cationic cages *via* the condensation of 3 equiv. of a bisamine linker with 1 equiv. of a hexaformyl compound, affording the desired products in near-quantitative yields. Within the framework of each cage, three acidic CH protons are oriented toward the interior cavity or the clefts, facilitating the accommodation of an-

* Corresponding author at: Department of Chemistry, Zhejiang University, Hangzhou 310058, China.
E-mail address: lihao2015@zju.edu.cn (H. Li).
[1] These authors contributed equally to this work.

https://doi.org/10.1016/j.cclet.2025.111554
1001-8417/© 2025 Published by Elsevier B.V. on behalf of Chinese Chemical Society and Institute of Materia Medica, Chinese Academy of Medical Sciences.

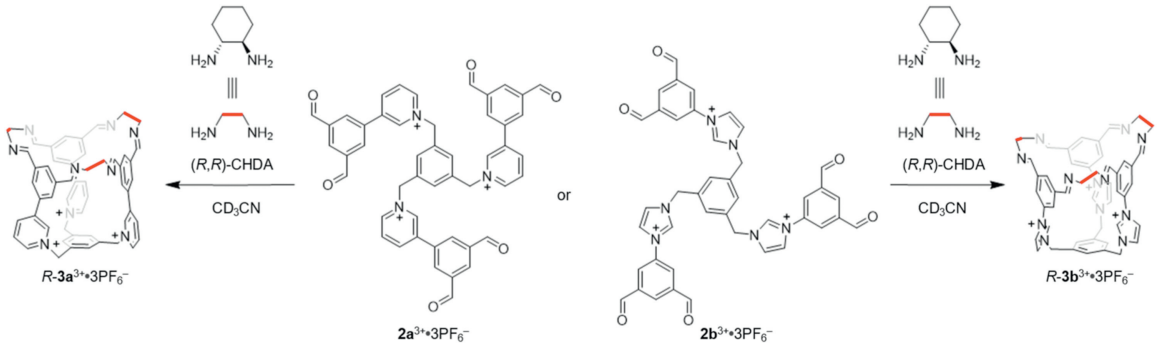


Fig. 1. Self-assembly of the cages *R*-**3a**$^{3+}$·3PF$_6^-$ and *R*-**3b**$^{3+}$·3PF$_6^-$ by condensing the hexaaldehyde precursor **2a**$^{3+}$·3PF$_6^-$ and **2b**$^{3+}$·3PF$_6^-$ and (1*R*,2*R*)-(-)-1,2-diaminocyclohexane ((*R*,*R*)-CHDA) in CD_3CN.

ionic guests through the formation of synergistic hydrogen bonds exhibiting modest binding affinities in both organic and aqueous media.

Two triscationic hexaaldehydes, **2a**$^{3+}$·3PF$_6^-$ and **2b**$^{3+}$·3PF$_6^-$, were synthesized *via* S_N2 reactions between tris(bromomethyl)benzene and the corresponding pyridine or imidazole precursors, followed by counterion exchange from bromide (Br^-) to hexafluorophosphate (PF_6^-). To construct the cage *R*-**3a**$^{3+}$, **2a**$^{3+}$·3PF$_6^-$ and (1*R*,2*R*)-(-)-1,2-diaminocyclohexane ((*R*,*R*)-CHDA) were combined in a 1:3 molar ratio in CD_3CN (Fig. 1).

The mixture was heated at 40 °C for at least 12 h, after which the ^{1}H NMR spectrum revealed a set of well-defined resonances corresponding to the formation of the cage molecule *R*-**3a**$^{3+}$. No significant byproducts were observed in the spectrum. Upon addition of tetrabutylammonium chloride ($TBA^+·Cl^-$) to the solution, *R*-**3a**$^{3+}$·3Cl$^-$ precipitated and was collected by filtration in 90% yield relative to the aldehyde precursor **2a**$^{3+}$·3PF$_6^-$. The isolated **3a**$^{3+}$·3Cl$^-$ was soluble in D_2O, and its ^{1}H NMR spectrum confirmed its stability in aqueous media, with no observable degradation during either counterion exchange or dissolution (Fig. S22 in Supporting information). Addition of ammonium hexafluorophosphate ($NH_4^+·PF_6^-$) to the aqueous solution resulted in the precipitation of *R*-**3a**$^{3+}$·3PF$_6^-$ in 95% yield relative to *R*-**3a**$^{3+}$·3Cl$^-$. Dissolving *R*-**3a**$^{3+}$·3PF$_6^-$ in CD_3CN yielded a ^{1}H NMR spectrum identical to that of the initial self-assembly solution, confirming the integrity of the cage structure (Fig. S17 in Supporting information). The enantiomer *S*-**3a**$^{3+}$·3Cl$^-$ and *S*-**3a**$^{3+}$·3PF$_6^-$ were synthesized following a similar procedure, using (*S*,*S*)-CHDA as the amino precursor. Similarly, analogous reactions using imidazolium-based precursor **2b**$^{3+}$ afforded *R*-**3b**$^{3+}$·3PF$_6^-$ and *R*-**3b**$^{3+}$·3Cl$^-$, as well as their enantiomers *S*-**3b**$^{3+}$·3PF$_6^-$ and *S*-**3b**$^{3+}$·3Cl$^-$. All cages were obtained in high yields, a result attributed to the dynamic nature of the imine bonds, which facilitates error correction during the self-assembly process.

The planar chirality of the cages is induced by the point chirality of the bisamino building blocks, specifically (*R*,*R*)-CHDA or (*S*,*S*)-CHDA. This chirality was confirmed through circular dichroism (CD) spectroscopy. In the CD spectra recorded in water, the cages *S*-**3a**$^{3+}$·3Cl$^-$ and *S*-**3b**$^{3+}$·3Cl$^-$ displayed (Fig. 2) mirror-image signals compared to their enantiomers, *R*-**3a**$^{3+}$·3Cl$^-$ and *R*-**3b**$^{3+}$·3Cl$^-$, respectively.

Diffraction-quality single crystals of *R*-**3a**$^{3+}$·3PF$_6^-$, *S*-**3a**$^{3+}$·3PF$_6^-$ and *R*-**3b**$^{3+}$·3PF$_6^-$ were successfully obtained by vapor diffusion of isopropyl ether into their respective acetonitrile solutions (CCDC 2363838, 2363601 and 2308786, respectively). The resulting solid-state structures unequivocally confirmed the formation of the cages (Fig. 3 and Fig. S118 in Supporting information). As anticipated, the frameworks of *R*-**3a**$^{3+}$ and *S*-**3a**$^{3+}$ are mirror images of each other, reflecting their enantiomeric relationship. In both

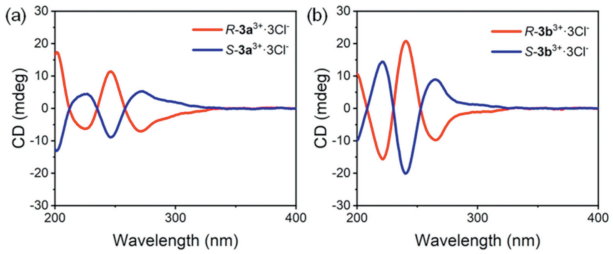


Fig. 2. CD spectra of *R*-**3a**$^{3+}$·3Cl$^-$ (red trace in (a)), *S*-**3a**$^{3+}$·3Cl$^-$ (blue trace in (a)), *R*-**3b**$^{3+}$·3Cl$^-$ (red trace in (b)) and *S*-**3b**$^{3+}$·3Cl$^-$ (blue trace in (b)). All spectra were recorded in water.

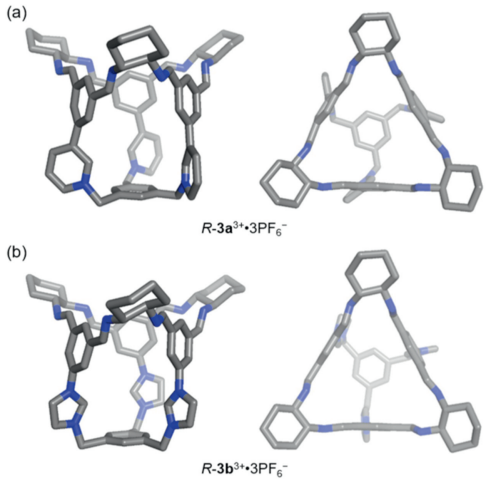


Fig. 3. Single-crystal X-ray diffraction structures of (a) *R*-**3a**$^{3+}$·3PF$_6^-$, (b) *R*-**3b**$^{3+}$·3PF$_6^-$. Carbon, grey; Nitrogen, blue. Disordered solvent molecules, hydrogen atoms and counterions are omitted for the sake of clarity.

the *R*/*S*-**3a**$^{3+}$ and *R*-**3b**$^{3+}$ frameworks, each pyridinium or imidazolium unit adopts an edge-in orientation. In the case of *R*-**3b**$^{3+}$, two of the three imidazolium units are oriented in a near perpendicular manner relative to the corresponding phenyl unit. As a consequence, the acidic imidazolium protons are directed toward the interior cavity. This conformation favors the formation of inclusion complexes, in which the anionic guest is located within the cage cavity. In the case of *R*-**3a**$^{3+}$, as a comparison, dihedral angle between each of the pyridinium unit and the corresponding phenyl unit is around 40°, indicating a *pseudo* face-in orientation. This conformation allows *R*-**3a**$^{3+}$ to accommodate guests in each of the three windows. This hypothesis is supported by the solid-state structure of *R*/*S*-**3a**$^{3+}$·3PF$_6^-$, in which the PF_6^- counteri-

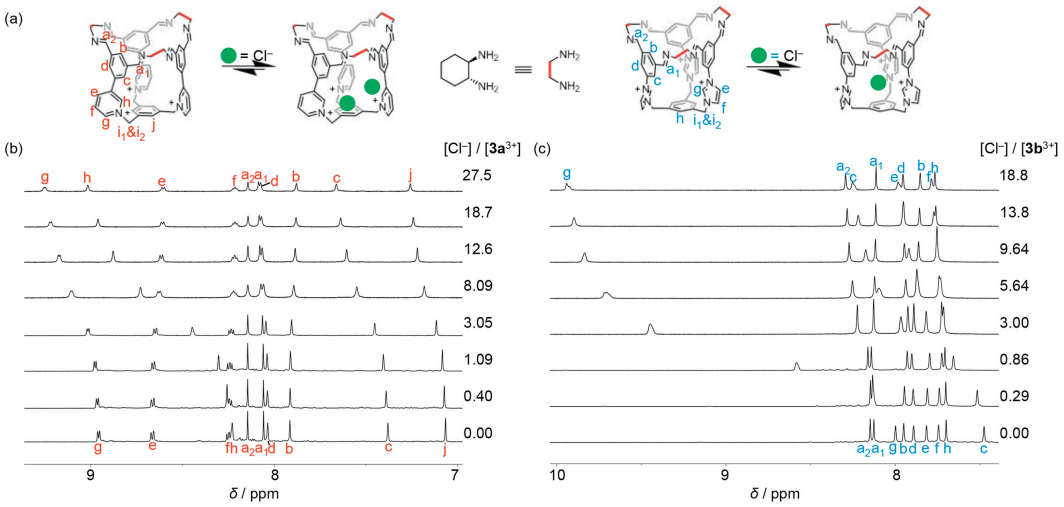


Fig. 4. (a) Schematic diagram of the different binding stoichiometries of $\mathbf{3a}^{3+}\cdot 3PF_6^-$ and $\mathbf{3b}^{3+}\cdot 3PF_6^-$ with Cl^-. Partial ^1H NMR spectra (600 MHz, CD_3CN, 298 K) of the cage (b) $\mathbf{3a}^{3+}\cdot 3PF_6^-$ and (c) $\mathbf{3b}^{3+}\cdot 3PF_6^-$ upon titration with different amounts of $TBA^+\cdot Cl^-$, till complete precipitation.

ons are located in the windows between the two pyridinium units. The cavity sizes of $\mathbf{3a}^{3+}\cdot 3PF_6^-$ and $\mathbf{3b}^{3+}\cdot 3PF_6^-$ were 135 Å^3 and 112 Å^3, respectively, calculated *via* GHECOM [35]. In the solid state, the cavities of both cages are devoid of any solvent molecules or PF_6^- counterions.

We then investigated the possibility of using the cages as acceptors to accommodate anions. First, based on the chiral nature of the cages, we investigated the recognition capabilities for chiral anions (*e.g.*, alanine or lactate). Unfortunately, no recognition was observed toward chiral anions, probably because none the chiral anionic guests had complementary size relative to the cage cavity. Therefore, we turned our attention to the achiral anions with smaller sizes such as halides. We evaluated the anion-binding capabilities of $\mathbf{3a}^{3+}$ and $\mathbf{3b}^{3+}$ in organic solvent, namely CD_3CN or CD_3SOCD_3. The ^1H NMR spectra of the cages before and after the addition of tetrabutylammonium salts ($TBA^+\cdot X^-$, X = Cl, Br, I and NO_3) were recorded and compared, indicating these anions were encapsulated within the cage cavities. For example, upon addition of $TBA^+\cdot Cl^-$ into a solution of $\mathbf{3a}^{3+}\cdot 3PF_6^-$ and $\mathbf{3b}^{3+}\cdot 3PF_6^-$ in CD_3CN, a number of resonances of the cage undergo shifts (Fig. 4). At the early stage of titration when Cl^- added was <3 equiv. relative to the hosts, the resonance corresponding to protons H_c and H_h of $\mathbf{3a}^{3+}$ and protons H_c and H_g of $\mathbf{3b}^{3+}$, which are directed toward the interior cavity, confirm that the anionic guests are recognized. The resonances corresponding to other protons that are located in relatively external positions in the cage framework underwent less remarkable shifts. These observations confirm that the anionic guests are recognized within the cage cavity, driven by hydrogen bonding interactions and electrostatic forces. In the case of $\mathbf{3b}^{3+}$, the shifts of resonances became less remarkable when the amount of Cl^- added is in excess. For example, the ^1H NMR spectra of $\mathbf{3b}^{3+}\cdot 3PF_6^-$ in the presence of 13.8 and 18.8 equiv. of $TBA^+\cdot Cl^-$ were similar (Fig. 4c), indicating that most of the host cavities are occupied by the anionic guest. As a comparison, in the case of $\mathbf{3a}^{3+}$, the saturation behavior did not occur even after adding 27.5 equiv. of Cl^- (Fig. 4b, top). It is noteworthy that the resonances corresponding to H_g and H_j, which barely shift in the early stage of anion titration, underwent downfield shift in the presence of excess Cl^-. This observation indicated that $\mathbf{3a}^{3+}$ might have multiple binding modes towards Cl^- during titration. That is, in the early stage of anion titration, the cage employed its cavity to recognize anionic guest, while in the late stage, the anions were recognized in a peripheral manner, leading to the shifts of the resonances corresponding to the external protons.

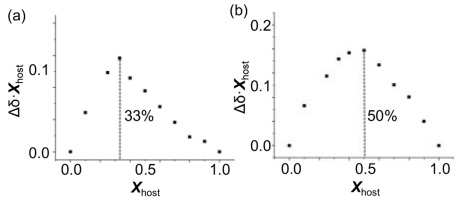


Fig. 5. Job plot of (a) $\mathbf{3a}^{3+}\cdot 3PF_6^-$ and (b) $\mathbf{3b}^{3+}\cdot 3PF_6^-$ to I^- made based on the corresponding ^1H NMR spectroscopic results in Supporting information.

Job plot analyses were conducted to determine the binding stoichiometry between the cages and anionic guests. The Job plot of $\mathbf{3a}^{3+}$ and $\mathbf{3b}^{3+}$ in CD_3CN revealed markedly distinct binding modes: $\mathbf{3a}^{3+}$ exhibited a 1:2 stoichiometry with all investigated anions, whereas $\mathbf{3b}^{3+}$ adopted a 1:1 binding ratio (Fig. 5). This difference is consistent with the NMR titration experiments, namely that $\mathbf{3b}^{3+}$ can only form the 1:1 inclusion complexes by using the cavity to encapsulate the anions, while $\mathbf{3a}^{3+}$ can form both inclusion and peripheral complexes by utilizing the windows as secondary binding sites.

The corresponding binding constants (K_a) were calculated *via* Bindfit. Using a 1:2 binding model might be more reasonable for $\mathbf{3a}^{3+}$. However, the attempt to do so only provided some unreliable secondary binding constants (K_{a2}), probably because the K_{a2} values are too small to be determined. We thus used the 1:1 binding model to calculate the K_a for both $\mathbf{3a}^{3+}\cdot 3PF_6^-$ and $\mathbf{3b}^{3+}\cdot 3PF_6^-$ in both CD_3CN and CD_3SOCD_3, which are summarized in Table 1. In the case of both cages, K_a values are significantly larger in CD_3CN compared to those in CD_3SOCD_3. For example, K_a was measured to be 1.5 ($\pm$0.1) $\times 10^3$ L/mol for the cage $\mathbf{3a}^{3+}$ to recognize Br^- in CD_3CN, while K_a was measured to be 1.0 ($\pm$0.1) $\times 10^2$ L/mol in CD_3SOCD_3, representing a decrease of more than one order of magnitude. This is predictable, given that more polar solvent, CD_3SOCD_3, helps to suppress both hydrogen bonding and electrostatic interactions. The apparent binding constants K_a of cage $\mathbf{3a}^{3+}$ for Br^- and I^- are significantly higher than those for Cl^-, while cage $\mathbf{3b}^{3+}$ shows slightly lower K_a values for Br^- and I^- compared to Cl^-. This is probably because cage $\mathbf{3b}^{3+}$ possesses a smaller cavity size compared to $\mathbf{3a}^{3+}$, while Br^- and I^- exhibit significantly larger ionic radii than Cl^- [36,37].

We also investigated the possibility of using $\mathbf{3a}^{3+}\cdot 3Cl^-$ and $\mathbf{3b}^{3+}\cdot 3Cl^-$ to recognize highly hydrated anions such as Cl^-, Br^- and

Table 1
Binding constants between two cages and anion guests in CD_3CN, CD_3SOCD_3 and D_2O.[a]

Host	Solvent	K_a (Cl^-) (L/mol)	K_a (Br^-) (L/mol)	K_a (I^-) (L/mol)	K_a (NO_3^-) (L/mol)
$\mathbf{3a}^{3+}\cdot 3PF_6^-$	CD_3CN	$8.7\ (\pm 0.1)\times 10^2$	$1.5\ (\pm 0.1)\times 10^3$	$1.4\ (\pm 0.1)\times 10^3$	$3.7\ (\pm 0.1)\times 10^2$
$\mathbf{3a}^{3+}\cdot 3PF_6^-$	CD_3SOCD_3	$1.2\ (\pm 0.1)\times 10^2$	$1.0\ (\pm 0.1)\times 10^2$	$7.2\ (\pm 0.1)\times 10^1$	$1.7\ (\pm 0.1)\times 10^2$
$\mathbf{3b}^{3+}\cdot 3PF_6^-$	CD_3CN	$4.8\ (\pm 0.3)\times 10^2$	$3.1\ (\pm 0.1)\times 10^2$	$2.0\ (\pm 0.1)\times 10^2$	$2.7\ (\pm 0.2)\times 10^2$
$\mathbf{3b}^{3+}\cdot 3PF_6^-$	CD_3SOCD_3	$2.3\ (\pm 0.1)\times 10^2$	$3.0\ (\pm 0.1)\times 10^2$	$1.8\ (\pm 0.1)\times 10^2$	$2.4\ (\pm 0.1)\times 10^2$
$\mathbf{3a}^{3+}\cdot 3Cl^-$	D_2O	N.D.[b]	$8.8\ (\pm\ 0.4)\times 10^1$	N.D.[c]	$1.6\ (\pm\ 0.3)\times 10^2$
$\mathbf{3b}^{3+}\cdot 3Cl^-$	D_2O	$1.7\ (\pm\ 0.1)\times 10^1$	$2.8\ (\pm\ 0.1)\times 10^1$	N.D.[c]	$1.6\ (\pm\ 0.1)\times 10^2$

[a] Initial attempts to fit the binding curve of $\mathbf{3a}^{3+}\cdot 3PF_6^-$ with anions using a 1:2 stoichiometric model proved unsuccessful, prompting the adoption of a 1:1 binding model which yielded an apparent binding constant K_a. $\mathbf{3a}^{3+}\cdot 3Cl^-$ and $\mathbf{3b}^{3+}\cdot 3Cl^-$ exhibit binding interactions with counterion Cl^- in D_2O, the binding constant K_a of $\mathbf{3a}^{3+}\cdot 3Cl^-$ and $\mathbf{3b}^{3+}\cdot 3Cl^-$ measured *via* titration corresponds to the apparent binding constant.
[b] K_a (Cl^-) of $\mathbf{3a}^{3+}\cdot 3Cl^-$ is too low to be determined.
[c] Addition of 1.0 equiv. of I^- causes complete precipitation, so K_a (I^-) of $\mathbf{3a}^{3+}\cdot 3Cl^-$ and $\mathbf{3b}^{3+}\cdot 3Cl^-$ cannot be determined.

NO_3^- in aqueous media. We attempted to obtain the Job plot in D_2O, but this approach failed due to the weak binding constant between the cage and anionic guest in D_2O [38]. However, the corresponding binding constants measured in water proved to be much weaker compared to those in organic media. For example, addition of NaCl into a solution of $\mathbf{3a}^{3+}\cdot 3Cl^-$ led to little or no shifts in the resonances of the cage, indicating the apparent binding constant K_a is too low to be determined (Fig. S104 in Supporting information). An alternative explanation, that the cavity of $\mathbf{3a}^{3+}$ is already occupied by a Cl^- ion due to an extraordinarily high K_a, is considered unlikely, as the K_a in CD_3CN is only $8.7\ (\pm 0.1)\times 10^2$ L/mol. Both cages exhibit modest K_a values for Br^- and NO_3^-. Attempts to determine the K_a value for I^- were unsuccessful, given that addition of I^- into the D_2O solutions of these two cages led to precipitation.

In summary, two sets of enantiomerically pure, cage-shaped molecules were successfully self-assembled in near-quantitative yields *via* dynamic imine condensation, bypassing the need for stepwise synthesis. Both cages demonstrate exceptional robustness, enabling their isolation as pure solid-state materials *via* counterion exchange without detectable degradation. The cationic building blocks, either pyridinium or imidazolium, adopt different conformations within the cage frameworks, namely that the imidazolium units are oriented in an edge-in manner, favoring the formation of an inclusion complex, while the pyridinium units are oriented in a *pseudo* face-in manner, allowing the cage to utilize both the cavity and the windows to accommodate anionic guests. As a consequence, the two cages respectively adopt distinct 1:1 and 1:2 binding stoichiometries. While binding affinities for highly hydrated anions remain modest in aqueous media, future efforts will focus on structural modifications, such as incorporating additional hydrogen bond donors or expanding cavity dimensions to accommodate larger guests. These investigations are currently underway in our laboratory.

Declaration of competing interest

The authors declare that they have no known competing financial interests or personal relationships that could have appeared to influence the work reported in this paper.

CRediT authorship contribution statement

Ze Cao: Writing – original draft, Validation, Methodology, Investigation, Formal analysis. **Chenqi Ge:** Supervision, Methodology, Investigation, Formal analysis. **Yating Wu:** Supervision. **Hua Tang:** Supervision. **Yueyan Kuang:** Supervision. **Yuyang Wu:** Supervision. **Hao Li:** Writing – review & editing, Supervision, Conceptualization.

Acknowledgments

The research at Zhejiang University was supported by the Starry Night Science Fund of Zhejiang University Shanghai Institute for Advanced Study (No. SN-ZJU-SIAS-006). H. L. Also want to thank the support from the Leading Innovation Team Grant from Department of Science and Technology of Zhejiang Province (No. 2022R01005), the Natural Science Foundation of Zhejiang Province (No. LZ24B020002) and the National Natural Science Foundation of China (No. 22471240). We thank Prof. Qiaohong He, Dr. Jiyong Liu, Dr. Yaqin Liu, Dr. Lina Gao and Dr. Yifan Zhao from the Chemistry Instrumentation Center Zhejiang University for the technical support.

Supplementary materials

Supplementary material associated with this article can be found, in the online version, at doi:10.1016/j.cclet.2025.111554.

References

[1] J. Zhu, Cell 167 (2016) 313–324.
[2] J.W.J.P. Ascher, Nature (1987) 529–531.
[3] H. Sies, D.P. Jones, Nat. Rev. Mol. Cell Biol. 21 (2020) 363–383.
[4] M.R. Awual, J. Clean. Prod. 228 (2019) 1311–1319.
[5] P. Loganathan, S. Vigneswaran, J. Kandasamy, J. Environ. Manage. 131 (2013) 363–374.
[6] B. Wu, J. Wan, Y. Zhang, et al., Environ. Sci. Technol. 54 (2020) 50–66.
[7] C.A. Cooper, J.M. Whittamore, R.W. Wilson, Am. J. Physiol. Regul. Integr. Comp. Physiol. 298 (2010) R870–R876.
[8] A.R.W.F. Boron, Physiol. Rev. 61 (1981) 296–434.
[9] D. Brown, C.A. Wagner, J. Am. Soc. Nephrol. 23 (2012) 774–780.
[10] L.R. Levin, J. Buck, Annu. Rev. Physiol. 77 (2015) 347–362.
[11] Y. Lei, L. Shen, J. Liu, et al., Chem. Commun. 55 (2019) 8297–8300.
[12] S. Lee, C. Chen, A.H. Flood, Nat. Chem. 5 (2013) 704–710.
[13] R. Cao, R.B. Rossdeutcher, Y. Zhong, et al., Nat. Chem. 15 (2023) 1559–1568.
[14] S. Niu, H. Xiao, X. Yang, et al., Chin. Chem. Lett. 34 (2023) 108042.
[15] K. Choi, A.D. Hamilton, J. Am. Chem. Soc. 125 (2003) 10241–10249.
[16] C.J. Pedersen, J. Am. Chem. Soc. 89 (1967) 7017–7036.
[17] R.M.I.P. Bruening, Chem. Rev. 91 (1991) 1721–2085.
[18] Y. Wu, C. Zhang, S. Fang, et al., Angew. Chem. Int. Ed. 61 (2022) e202209078.
[19] H. Sunohara, K. Koyamada, H. Takezawa, et al., Chem. Commun. 57 (2021) 9300–9302.
[20] W. Lin, G. Zhang, X. Zhu, et al., J. Am. Chem. Soc. 145 (2023) 12609–12616.
[21] H. Wang, S. Fang, G. Wu, et al., J. Am. Chem. Soc. 142 (2020) 20182–20190.
[22] A.J. Plajer, E.G. Percástegui, M. Santella, et al., Angew. Chem. Int. Ed. 58 (2019) 4200–4204.
[23] Y. Chen, G. Wu, L. Chen, et al., Org. Lett. 22 (2020) 4878–4882.
[24] W. Jiang, B. Huang, X. Zhao, et al., Chem 9 (2023) 2655–2668.
[25] W.Z.C.C. Yun Liu, Science 365 (2019) 159–161.
[26] J. Wu, J.L. Greenfield, J. Am. Chem. Soc. 146 (2024) 20720–20727.
[27] S. Jiang, J.T.A. Jones, T. Hasell, et al., Nat. Commun. 2 (2011) 207.
[28] H. Li, H. Zhang, A.D. Lammer, et al., Nat. Chem. 7 (2015) 1003–1008.
[29] C. Ge, Z. Cao, T. Feng, et al., Angew. Chem. Int. Ed. 63 (2024) e202411401.
[30] T. Jiao, L. Chen, D. Yang, et al., Angew. Chem. Int. Ed. 56 (2017) 14545–14550.
[31] P. Jacques, V. Artero, J. Pecaut, et al., Proc. Natl. Acad. Sci. U. S. A. 106 (2009) 20627–20632.
[32] A. Dirksen, S. Dirksen, T.M. Hackeng, et al., J. Am. Chem. Soc. 128 (2006) 15602–15603.
[33] S. Zhao, M.M. Abu-Omar, Macromolecules 51 (2018) 9816–9824.
[34] Y. Lei, Q. Chen, P. Liu, et al., Angew. Chem. Int. Ed. 60 (2021) 4705–4711.
[35] T. Kawabata, Biophys. Physicobiol. 16 (2019) 391–406.
[36] A.M. Miguel Ponce-Vargas, Phys. Chem. Chem. Phys. 17 (2015) 18677–18683.
[37] V.C.P.C. Camila Munoz Zuniga, G.F.C.A. Renato, L.T. Parreira, J. Phys. Chem. C 128 (2024) 14017–14024.
[38] K.D.T.B. Filip Ulatowski, J. Org. Chem. 81 (2016) 1746–1756.